EDGE ARTICLE

Check for updates

An isocyanide ligand for the rapid quenching and efficient removal of copper residues after Cu/TEMPO-catalyzed aerobic alcohol oxidation and atom transfer radical polymerization†

Grzegorz Szczepaniak, [ID] *[ab] Jakub Piątkowski, [ID] ‡[a] Wojciech Nogaś, [ID] ‡[a]
Francesca Lorandi, [ID] ‡[b] Saigopalakrishna S. Yerneni,[c] Marco Fantin, [ID] [b]
Anna Ruszczyńska, [ID] [a] Alan E. Enciso,[d] Ewa Bulska, [ID] [a] Karol Grela [ID] *[a]
and Krzysztof Matyjaszewski [ID] *[b]

Transition metal catalysts play a prominent role in modern organic and polymer chemistry, enabling many transformations of academic and industrial significance. However, the use of organometallic catalysts often requires the removal of their residues from reaction products, which is particularly important in the pharmaceutical industry. Therefore, the development of efficient and economical methods for the removal of metal contamination is of critical importance. Herein, we demonstrate that commercially available 1,4-bis(3-isocyanopropyl)piperazine can be used as a highly efficient quenching agent (**QA**) and copper scavenger in Cu/TEMPO alcohol aerobic oxidation (Stahl oxidation) and atom transfer radical polymerization (ATRP). The addition of **QA** immediately terminates Cu-mediated reactions under various conditions, forming a copper complex that can be easily separated from both small molecules and macromolecules. The purification protocol for aldehydes is based on the addition of a small amount of silica gel followed by **QA** and filtration. The use of **QA@SiO$_2$** synthesized *in situ* results in products with Cu content usually below 5 ppm. Purification of polymers involves only the addition of **QA** in THF followed by filtration, leading to polymers with very low Cu content, even after ATRP with high catalyst loading. Furthermore, the addition of **QA** completely prevents oxidative alkyne–alkyne (Glaser) coupling. Although isocyanide **QA** shows moderate toxicity, it can be easily converted into a non-toxic compound by acid hydrolysis.

Introduction

The goal of synthetic chemistry is to efficiently produce diverse compounds of high purity. Since many important synthetic transformations require the use of transition metal catalysts,[1–6] the problem of purifying the products from metal residues is of considerable practical importance. A metal impurity can promote the decomposition of the desired product or compromise the performance of advanced materials.[7,8] Additionally, transition metal-catalyzed reactions are used in the large scale synthesis of modern active pharmaceutical ingredients (API).[9–11] Therefore, this issue is crucial in the pharmaceutical industry, which is subject to stringent limits on the allowed concentration of heavy metals in the final API, typically less than 10 ppm. Traditional separation methods, such as chromatography or crystallization, often fail to give products with acceptably low metal content, especially when applied to compounds with functional groups that can bind to transition metals.[12]

In recent years, more attention has been given to tackling the problem of metal contamination as early as possible in the synthetic pipeline.[13] Possible approaches include heterogeneous catalysis, self-scavenging catalysts, and the use of metal scavengers.[14,15] In 2015, inspired by the work of Diver and co-workers,[16] we reported a new, stable, odorless, bidentate isocyanide scavenger and quenching agent **QA** (1,4-bis(3-isocyanopropyl)piperazine),[17] which was used to remove ruthenium impurities from olefin metathesis products and

[a]Faculty of Chemistry, Biological and Chemical Research Centre, University of Warsaw, Żwirki i Wigury 101, 02-089 Warsaw, Poland. E-mail: szczepaniak.grzegorz@gmail.com; prof.grela@gmail.com

[b]Department of Chemistry, Carnegie Mellon University, 4400 Fifth Avenue, Pittsburgh, Pennsylvania 15213, USA. E-mail: km3b@andrew.cmu.edu

[c]Department of Biomedical Engineering, Carnegie Mellon University, Pittsburgh, Pennsylvania, USA

[d]Department of Chemistry, Northwestern University, 2145 Sheridan Road, Evanston, Illinois 60208, USA

† Electronic supplementary information (ESI) available. See DOI: 10.1039/d0sc00623h

‡ These authors contributed equally.

palladium residues from cross-coupling products by straightforward purification protocols.[17–19]

Copper-based catalysts are used in many transformations of critical importance to both laboratory and industrial applications,[20] including azide–alkyne Huisgen cycloaddition (CuAAC),[21] atom transfer radical polymerization (ATRP),[22] Ullmann coupling,[23] and aerobic oxidation reactions.[24] Since isocyanide ligands can coordinate to late 4d and 5d transition metals due to their σ-donor and π-acceptor properties,[25] we hypothesized that **QA** could be used as a copper scavenger in the purification of Cu/TEMPO alcohol aerobic oxidation (Stahl oxidation) products and also for polymers made by Cu-catalyzed ATRP. The results presented in this study validate this hypothesis and show that **QA** could be used to purify both small molecules and macromolecules from copper impurities. In addition, **QA** immediately stops copper-mediated reactions, facilitating kinetic studies, and reaction design. Finally, we demonstrated that **QA** could be used to prevent side reactions, such as Glaser coupling, that can occur during polymers workup.

Alcohol oxidation is one of the most widely used oxidation reactions in the synthesis of complex organic molecules. In recent years, aerobic oxidation reactions have been the focus of considerable attention.[26,27] Compared to traditional reagents and methods, these transformations are attractive due to the use of molecular oxygen as an inexpensive oxidant. Furthermore, aerobic oxidation is an environmentally benign method characterized by lower process mass intensity (PMI) compared to traditional alcohol oxidation protocols such us Swern,[28] Parikh–Doering oxidation[29] and TEMPO/NaOCl (TEMPO = 2,2,6,6-tetramethylpiperidine N-oxyl) based methods.[30,31]

The Stahl group developed a highly practical, selective, mild and efficient aerobic alcohol oxidation mediated by the Cu/TEMPO system,[32–34] which exhibits high functional group tolerance and has found many applications in organic synthesis.[26,35–37] However, to the best of our knowledge, there has been no study on the removal of copper residues for this type of transformation.
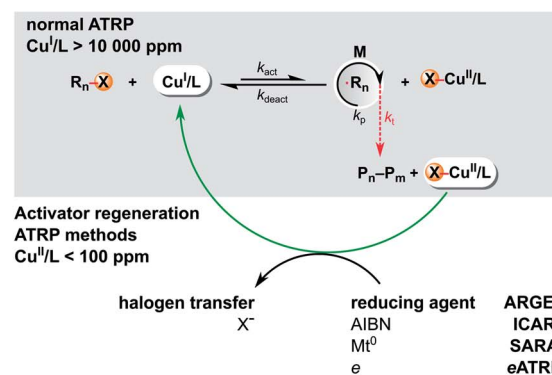
The catalytic cycle for Cu/TEMPO-catalyzed aerobic alcohol oxidation involves oxidation of Cu^I/L complex by molecular oxygen to a peroxo-bridged binuclear Cu^{II} intermediate (Scheme 1A). The [Cu^{II}/L]$_2$O$_2$ species oxidize the hydroxylamine (TEMPOH = 2,2,6,6-tetramethylpiperidin-1-ol) to TEMPO, leading to the formation of a HOO–Cu^{II}/L and a Cu^I/L complex. Then, the HOO–Cu^{II}/L intermediate reacts with water to afford a HO–Cu^{II}/L and hydrogen peroxide. Finally, the OH–Cu^{II}/L and TEMPO mediate the oxidation of alcohol via a six-membered transition state, resulting in aldehyde formation and regeneration of Cu^I/L complex.[38]

Atom transfer radical polymerization (ATRP) is now considered one of the stock transformations in the toolbox of modern polymer chemistry.[22,39–41] Due to its compatibility with a wide variety of functional groups, easy setup, and mild conditions, it is used in a wide range of applications. ATRP is based on a reversible redox reaction catalyzed by transition metal complexes in their lower oxidation state. The most common ATRP catalysts are Cu complexes.[42]
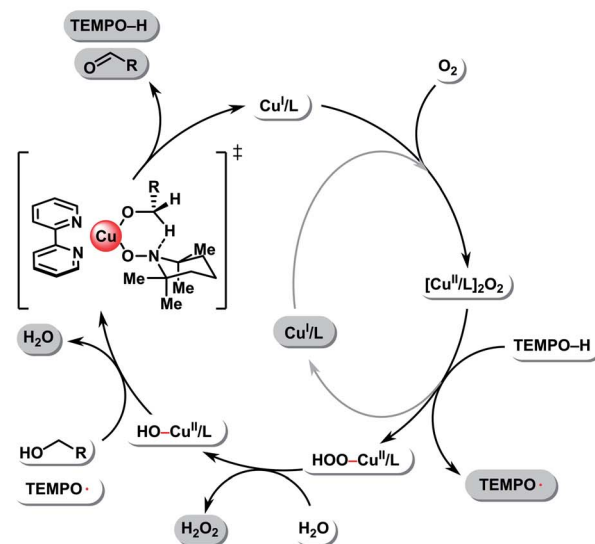
Scheme 1 (A) Mechanism of Cu/TEMPO alcohol aerobic oxidation (Stahl oxidation). (B) Mechanism of Cu-catalyzed normal ATRP and low-ppm ATRP in the presence of excess reducing agents.

The control over radical propagation in ATRP is provided via an atom transfer equilibrium between a Cu^I/L and a X–Cu^{II}/L complex, where L represents a multidentate nitrogen-based ligand and X is a halogen (Scheme 1B). The Cu^I/L complex activates the C(sp^3)–X polymer chain end, resulting in the formation of a propagating carbon-based radical and the deactivator form (X–Cu^{II}/L) of the catalyst. Then, the X–Cu^{II}/L reacts with the propagating radical in a reverse reaction, regenerating the active catalyst Cu^I/L and the dormant polymer chain end C(sp^3)–X.[22]

Standard ATRP requires a large amount of an oxygen sensitive Cu^I/L catalyst (>10 000 ppm with respect to the monomer),[43,44] the residues of which are difficult to remove from the polymer (Scheme 1B). Recently, several new ATRP techniques were developed to overcome this (Scheme 1B). They are based on the regeneration of the active form of the catalyst using various external stimuli, which allows reducing the catalyst loading to less than 100 ppm. These methods include: activators generated by electron transfer (AGET),[45] activators regenerated by electron transfer (ARGET),[46] initiators for continuous activator

regeneration (ICAR),[47] supplemental activators and reducing agent (SARA),[48] electrochemically mediated ATRP (eATRP),[49] photoinduced ATRP (pATRP),[50] and mechanically/ultrasound induced ATRP (mechano/sonoATRP).[51,52]

The ideal approach to overcoming copper contamination in traditional ATRP systems is the recently developed metal-free ATRP, catalyzed by an organic photoredox catalyst.[53–56] However, the narrow monomer scope is a major limitation of this technique. Moreover, it creates a new challenge – the product can be contaminated with the organocatalyst.

Despite significant progress in the development of ATRP techniques, many modern applications that give access to complex macromolecular architectures still require the use of high loadings of copper catalysts.[57] Moreover, in biomedical applications, copper residues in polymers can induce cellular oxidative damage.[58] For these reasons, the development of economical and practical methods for the removal of copper impurities after ATRP is highly desirable.

The problem of copper contamination in polymers can be solved by precipitation, dialysis, extraction, or filtration through a silica gel or aluminum oxide. Unfortunately, standard polymer purification protocols are often insufficient to bring the copper content below 10 ppm, in particular when polymers exhibit high affinity towards copper.[59] To address this issue, many advanced methods of purification have been developed,[60,61] including heterogeneous catalysis,[62–64] self-scavenging catalysts,[65–67] metal scavengers,[68] switchable systems,[69] ion-exchange resins,[70] electrolysis of copper residues[59,71] and other related electrochemical methods to reduce copper.[72] However, most of these purification protocols suffer from at least one critical flaw, such as complexity and limited availability, the need of specialized equipment, long purification time, issues with end-group fidelity or inability to decrease the copper content below 10 ppm.

Herein, we demonstrate that the introduction of the quenching agent QA rapidly stops ATRP under various conditions, forming a copper complex that precipitates, allowing for facile removal by filtration. After this treatment, the residual copper contamination of the polymers was <2 ppm, even when a high initial catalyst loading was used. Similarly, the addition of QA to Stahl oxidation products decreased the copper content below 5 ppm.

Results and discussion

Quenching of Stahl oxidation by isocyanide QA

We started our investigation by examining QA as a quenching agent of Stahl oxidation (Fig. 1A). Our hypothesis assumed that QA might form a stable complex with copper(I) that does not oxidize further. Aerobic oxidation of nerol (1a) was performed in MeCN at room temperature, in a reaction vessel open to the air, with CuI/bpy/TEMPO/DMAP (bpy = 2,2′-bipyridine, DMAP = 4-(dimethylamino)pyridine) as the catalytic system. After 24 h, in the presence of QA, the conversion of alcohol 1a was 0% (Fig. 1A), while in the control experiment without the addition of QA, it was >99%. These experiments showed that isocyanide QA is binding to copper, inhibiting the oxidation reaction.
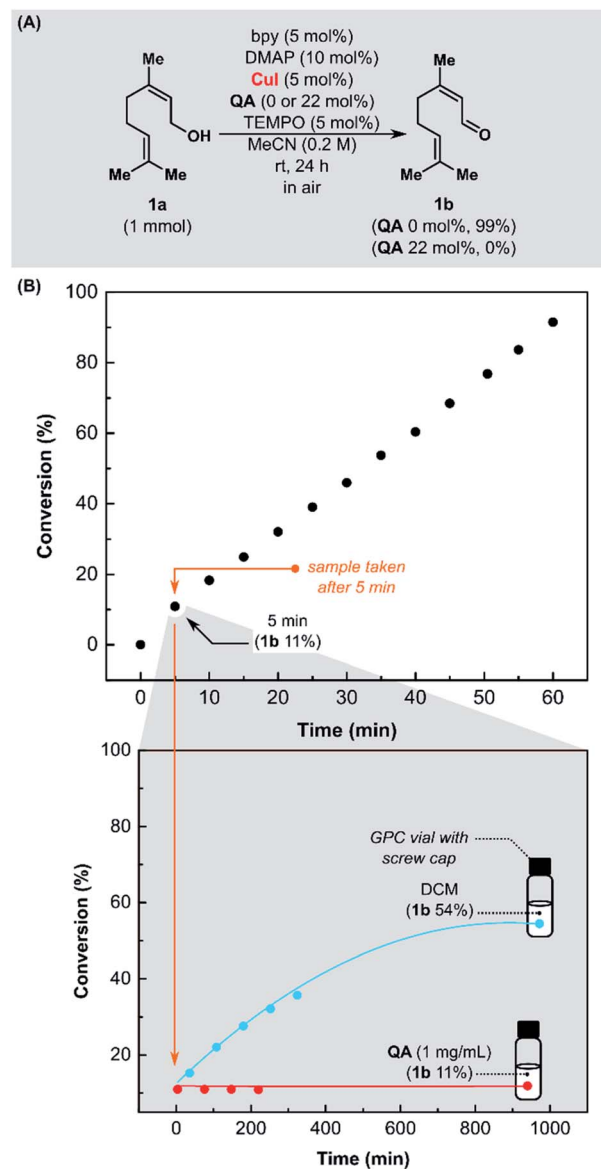

Fig. 1 (A) Quenching of Stahl oxidation by QA. (B) Evaluation of the performance of QA as a quenching agent in Stahl oxidation of nerol (1a), reaction conditions: 1a (1 mmol), bpy (5 mol%), DMAP (10 mol%), CuI (5 mol%), TEMPO (5 mol%).

Next, we evaluated the performance of QA as a quenching agent in the Cu-catalyzed oxidation of 1a. The kinetic study was performed at room temperature in a reaction vessel open to the air, using CuI/bpy/TEMPO/DMAP catalytic system (Fig. 1B). Aliquots of the reaction mixture (0.2 mL) were added to a solution of QA in DCM (1.0 mL, 1 mg mL^{-1}) at selected time and then analyzed with gas chromatography (GC).

After 5 min, a sample was taken from the reaction mixture. Half of it was added to a solution of scavenger QA in DCM, and the remainder was added to pure DCM (Fig. 1B). Even though the reaction mixture was significantly diluted and the access to air was limited (vial with screw cap), the oxidation of alcohol 1a was still proceeding (blue curve). In the vial containing QA, the conversion did not change over time (red curve).
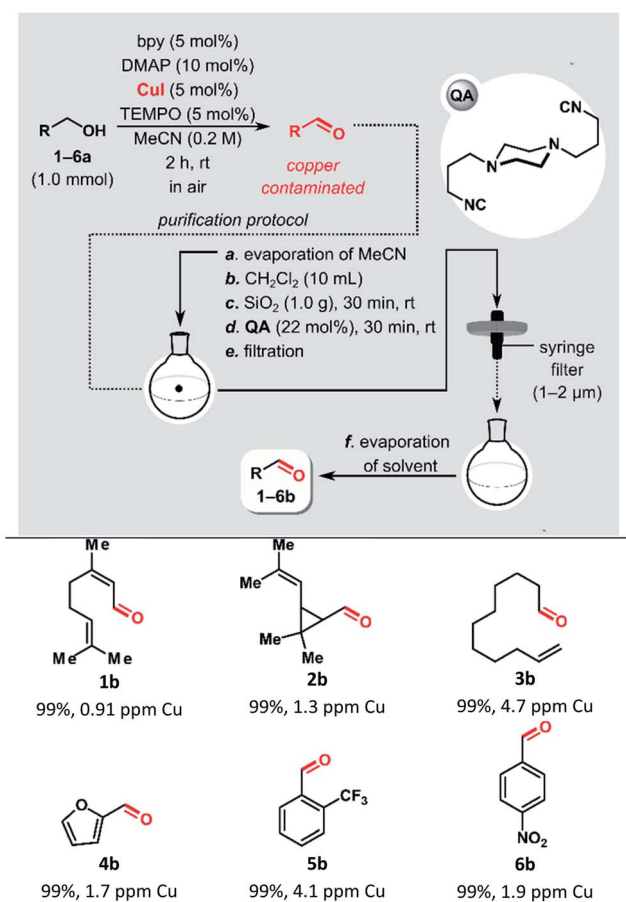
Then, we examined the activity of various copper catalytic systems utilizing **QA** (Fig. 1S†). This study demonstrated that **QA** could be used as a fast-acting quenching agent to facilitate the kinetic studies of Cu-mediated oxidation of alcohols by halting the reaction progress at a specific point in time and using an offline analytic method, such as GC, to analyze the samples.[73] To the best of our knowledge, no quenching agent for this transformation has yet been described in the literature. To determine the conversion as a function of time by GC, it was necessary to conduct an independent experiment for every time interval and terminate it by filtration through silica gel.[74] The proposed quenching method is fast and easy to carry out. Encouraged by these promising results, we evaluated **QA** as a metal scavenger in the removal of copper residues.

Removal of copper residues after Stahl Oxidation

Recently, we reported a semi-heterogeneous purification protocol for the removal of ruthenium impurities after olefin metathesis reaction.[19] It is based on the noncovalent immobilization of **QA** on unmodified silica gel during the purification

process. Herein, we applied this protocol to the removal of copper residues after Cu-mediated oxidation of alcohols.

For the evaluation of **QA** performance in the removal of copper impurities after Stahl oxidation, we selected aliphatic and aromatic alcohols with different functional groups (Table 1). All reactions used 1.0 mmol of the alcohol and were performed in MeCN at room temperature with ambient air as the source of oxidant, using a CuI/bpy/TEMPO/DMAP catalytic system. After 2 h, the conversions for all tested substrates were >99%.

To minimize the risk of leaching the copper-containing contaminants from the silica gel, MeCN was evaporated before removing the copper, and then DCM was added. The solvent switch can be avoided. However, the best results were obtained when MeCN was removed before the purification (ESI Table S1†). The addition of silica gel, followed by the isocyanide treatment, allowed for isolating aldehydes with very low copper content, below 5 ppm. Meanwhile, a control experiment with furfural (**4b**), in which no **QA** was added, yielded a product that remained contaminated with copper at a very high level, 800 ppm. In
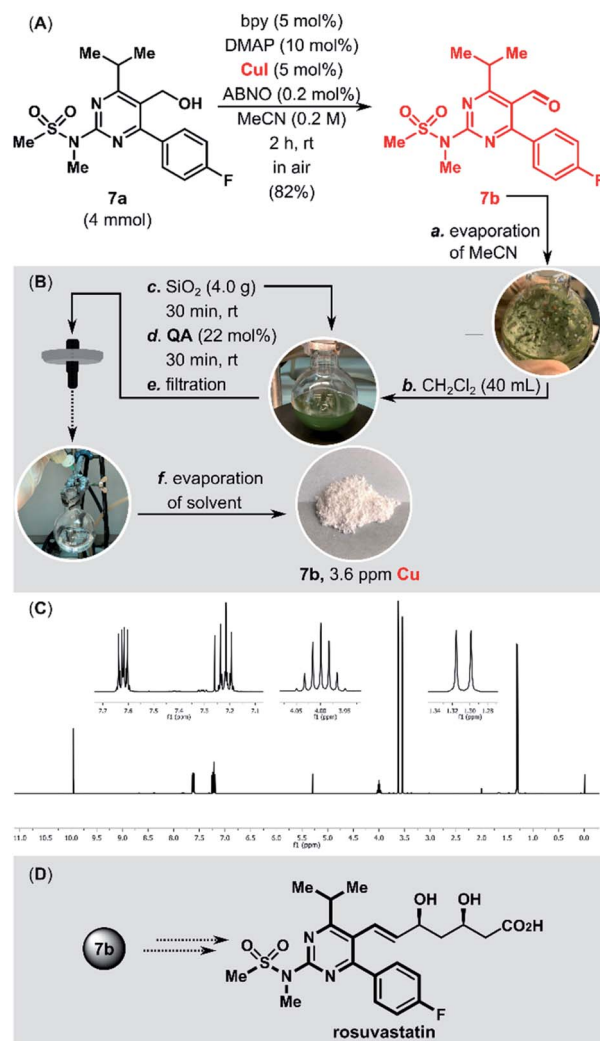
Table 1 Removal of Cu residues after Stahl oxidation[a]

[a] Conversions were determined by GC analysis and are based on the ratio of product/(product + starting material). Cu content was determined by ICP-MS.

Fig. 2 (A) Stahl oxidation of the rosuvastatin precursor (**7a**) on a gram scale. (B) Removal of Cu residues from **7b**. (C) ¹H NMR spectrum of **7b** after purification. (D) Rosuvastatin structure.

addition, since most of the catalytic system components bind strongly to silica gel after simple filtration through a syringe filter, followed by evaporation of the solvent, the isolated products were pure, based on ^{1}H NMR spectroscopic analysis.

Cu/TEMPO catalyst systems show reduced reactivity with aliphatic and sterically hindered alcohols. Stahl and co-workers demonstrated that replacement of TEMPO with the less sterically hindered ABNO (ABNO = 9-azabicyclo[3.3.1]nonane N-oxyl) diminishes the steric and electronic constraints of the Cu/TEMPO.[75] The aerobic oxidation of the sterically hindered alcohol **7a** in a gram scale (4 mmol, 1.41 g) was performed using the highly active CuI/bpy/ABNO/DMAP catalytic system (Fig. 2). The new purification protocol proved to be scalable. After purification, the copper content in the isolated aldehyde **7b**, a key intermediate in the synthesis of cardiovascular disease drug rosuvastatin,[76] was only 3.6 ppm.

Reactivity of QA toward ATRP catalysts

The promising results on the removal of copper residues after Stahl oxidation prompted us to utilize **QA** in ATRP. First, we examined **QA** reactivity towards benchmark ATRP Cu[II]-catalysts. Nitrogen-based polydentate ligands commonly used in Cu-mediated ATRP have strong σ-donor properties,[77] which ensure effective coordination of the ligand to copper in both oxidation states. However, for ATRP ligands, the stability constant β^{II} (binding constant for Cu[II]) is much higher than β^{I} (binding constant for Cu[I]), providing a thermodynamic driving force for the activation of C(sp[3])–X bonds. β^{II} values ranging from 10^{18} to 10^{27} M^{-1} and corresponding β^{I} between 10^{7} and 10^{13} M^{-1} have been reported for conventional ATRP catalysts in organic solvents.[78] The first question we had to answer was whether **QA** could form a complex with Cu[II] in the presence of strong σ-donor ligands.

To test the performance of **QA**, its reaction with [Cu[II](TPMA)Br]$^{+}$ (TPMA = tris(2-pyridylmethyl)amine) was performed in DMSO under ambient atmosphere (Fig. 3). The progress of the reaction was monitored by UV-vis spectroscopy. After the addition of **QA** (4 equiv.) to [Cu[II](TPMA)Br]$^{+}$, no ligand exchange occurred in the coordination sphere of copper (Fig. 3B). For Me$_6$TREN (Me$_6$TREN = tris[2-(dimethylamino)ethyl]amine) and PMDETA (PMDETA = N,N,N′,N″,N″-pentamethyldiethylenetri-amine) ligand, the results were similar (ESI Fig. S2 and S3†). However, the addition of ascorbic acid (**AA**) in excess (10 equiv.) resulted in the immediate replacement of TPMA with **QA**. The absorption band of [Cu[II](TPMA)Br]$^{+}$ immediately disappeared in the UV-vis spectrum (Fig. 3C). Conversely, the addition of **AA** alone did not cause any changes in the spectrum (ESI Fig. S4B†).

Ascorbic acid reduces Cu[II] to Cu[I], which results in a swift reaction between the [Cu[I](TPMA)]$^{+}$ complex and the isocyanide **QA**, even though atmospheric oxygen is present in the system (Fig. 4C). In the absence of **QA**, the atmospheric oxygen immediately oxidizes [Cu[I](TPMA)]$^{+}$. Therefore, the UV-vis spectrum does not show any changes after the addition of **AA** (ESI Fig. S4B†). Due to their strong σ-donor properties and their weak π-acidity, isocyanides preferentially bind to transition metals in a low oxidation state.[25] As expected, the compound **QA** has very high affinity to Cu[I]/L and does not react with Cu[II]/L with electron-rich ligands that strongly bind to Cu[II].

Similar conclusions can be drawn from the experiment where the complex [Cu[II](TPMA)Br]$^{+}$ was reduced by compro-portionation with Cu(0) in the presence of excess **QA** under anaerobic conditions in DMSO (Fig. 4). In the presence of **QA**, a white solid precipitated as the copper comproportionation
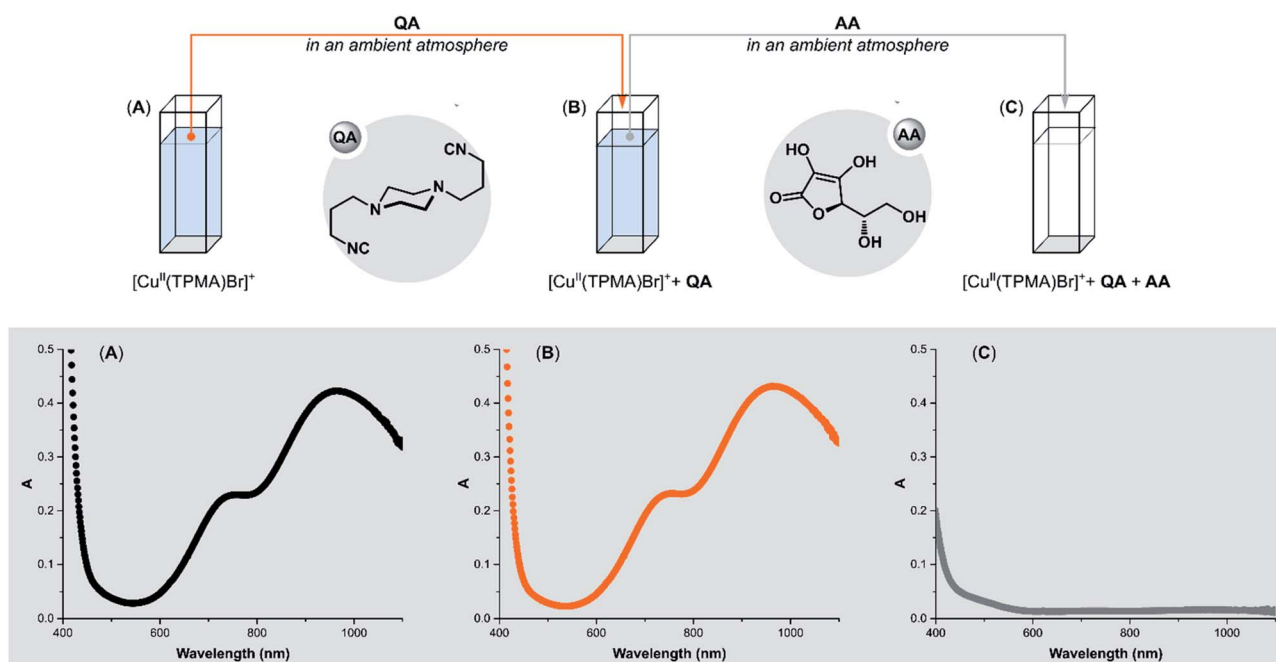

Fig. 3 QA reactivity towards the [Cu[II](TPMA)Br]$^{+}$. (A) UV-vis spectra of [Cu[II]Br$_2$] = 2.5 mM; [TPMA] = 2.5 mM in DMSO at 22 °C in air. (B) UV-vis spectra of copper complex after addition of QA (4 equiv.). (C) UV-vis spectra of copper complex after addition of QA (4 equiv.) and AA (10 equiv.).
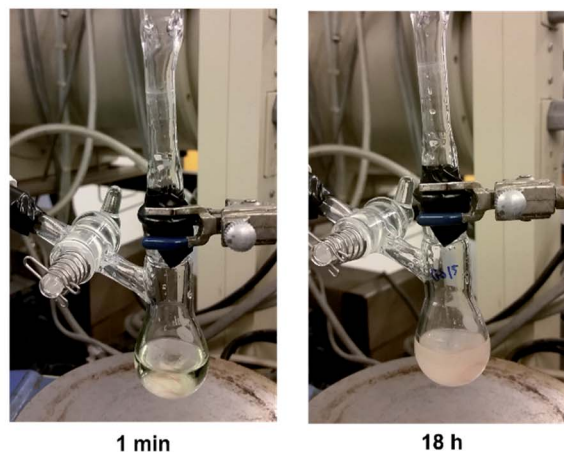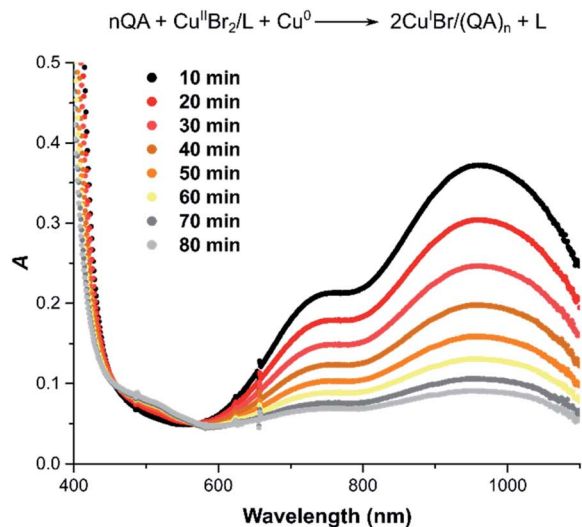
$$nQA + Cu^{II}Br_2/L + Cu^0 \longrightarrow 2Cu^IBr/(QA)_n + L$$

Fig. 4 Comproportionation of $[Cu^{II}Br_2] = 2.5$ mM with $[TPMA] = 5.25$ mM in the presence of $[QA] = 10.0$ mM and 4 cm Cu(0) wire ($d = 1$ mm, $S = 1.27$ cm^2); in DMSO at 22 °C.

proceeded. After 18 hours, the reaction mixture was exposed to air and filtered through a syringe filter. The UV-vis spectrum showed the complete disappearance of the Cu^{II}/L complex (ESI Fig. S5A†). The same result was recorded after 19 hours of air exposure, indicating that the Cu^I bound to **QA** ligand was not re-oxidized to Cu^{II} (ESI Fig. S5B†). In the control experiment in which no **QA** was added, $[Cu^I(TPMA)]^+$ was oxidized (ESI Fig. S6†). These experiments have shown that **QA** can quantitatively bind to the Cu^I generated by the action of a reducing agent, even in the presence of strong σ-donor ligands, to form air-stable, polar copper(ı) complexes with **QA**.

These results were confirmed by electrochemical analysis. Cyclic voltammetry (CV) is commonly used to investigate the reactivity of ATRP catalysts,[79] which typically exhibit a quasi-reversible voltammetric behavior (*e.g.*, Fig. 5, black line). There-fore CV was used to analyze the effect of **QA** on $[Cu^{II}(TPMA)Br]^+$ in DMSO. When a relatively small amount of **QA** was present (<0.5 equiv.), a new cathodic peak appeared, shifted at more positive

potentials compared to the cathodic peak of $[Cu^{II}(TPMA)Br]^+$. While the latter gradually decreased in intensity, a more pronounced decrease was observed in the intensity of the anodic peak, corresponding to the re-oxidation of $[Cu^I(TPMA)Br]$ to $[Cu^{II}(TPMA)Br]^+$. A new broad oxidation peak appeared at more positive potentials. When the concentration of **QA** was increased, only the cathodic peak at more positive potentials was detected. Its intensity slightly decreased when the amount of **QA** was increased. No oxidation peak could be recorded when ≥1 equiv. of **QA** was present. The described behavior is consistent with the occurrence of a fast and irreversible chemical reaction following the electron transfer process,[80] which results in the shift of the voltammetric signal to more positive potential values. In our experiment, **QA** reacted with the Cu^I species that was generated in the vicinity of the electrode during the potential scan. This reaction rendered the reduction of $[Cu^{II}(TPMA)Br]^+$ to $[Cu^I(TPMA)Br]$ more favorable, thus shifting its potential to more positive values. Moreover, **QA** formed a stable species with the copper(ı) complex (at least in the timescale of CV), and therefore the cathodic peak corresponding to the re-oxidation of $[Cu^I(TPMA)Br]$ decreased in intensity and then disappeared for relatively high amounts of **QA**. The fact that no other peaks ware detected in the explored potential range supports the formation of a non-electroactive complex between Cu(ı) and **QA** (*i.e.* that cannot be oxidized), which is therefore unable to catalyze Stahl oxidation or ATRP reactions.

The CV experiment supported the ability of **QA** to strongly bind to Cu^I species. However, one can expect a similar voltammetric response both when **QA** binds to Cu^I/L and when it displaces the ligand and binds to "naked" Cu^I. One possibility to discriminate between these two scenarios is to look at a more positive potential range in a similar CV experiment. When the amount of **QA** increased, several anodic signals appeared or increased in intensity at $E > 0.8$ V *vs.* SCE, which could be ascribed to the oxidation of free Br$^-$ anions and TPMA (ESI Fig. S7†). This suggested that TPMA was at least partially displaced by **QA**.
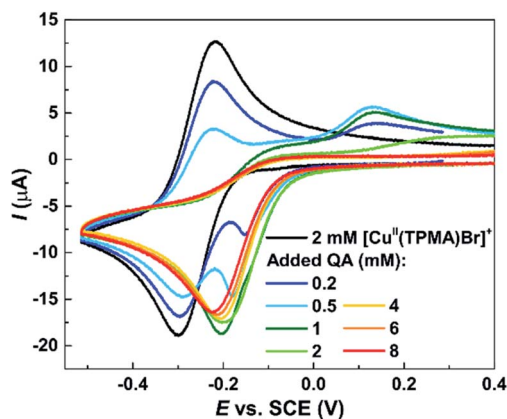

Fig. 5 Cyclic voltammetry of 2 mM $[Cu^{II}(TPMA)Br]^+$ in DMSO + 0.1 M Et$_4$NBF$_4$, in the absence and in the presence of QA. Scan rate = 0.2 V s^{-1}, $T = 25$ °C.
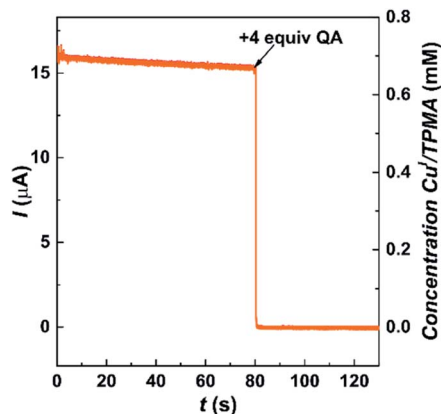
Fig. 6 Decay of limiting current *vs.* time for the reaction between 0.7 mM $[Cu^I(TPMA)]^+$ and 2.8 mM **QA** in DMSO + 0.1 M Et_4NBF_4, recorded at $E_{app} = 0.29$ V *vs.* SCE on a RDE, $l = 4000$ rpm, $T = 25$ °C.

A rotating disk electrode (RDE) was used to directly observe the effect of **QA** on $[Cu^I(TPMA)]^+$ in DMSO. Chronoamperometry under hydrodynamic conditions was used to monitor the concentration of $[Cu^I(TPMA)]^+$ by applying a potential of 0.29 V *vs.* SCE (Fig. 6). Initially, only $[Cu^I(TPMA)]^+$ was present in the solution and a slowly decreasing limiting current was recorded due to the slow disproportionation of the complex. When 4 equiv. of **QA** were added, the current immediately dropped to zero, indicating that no $[Cu^I(TPMA)]^+$ remained in the solution. If only a stoichiometric amount of **QA** was added, the current did not drop to zero but to a small value (ESI Fig. S8A†),[81] indicating that an excess of **QA** was needed to effectively bind to all Cu^I species. Nevertheless, the current drop was instantaneous, both for $[Cu^I(TPMA)]^+$ and for a Cu^I complex with 3 orders of magnitude higher ATRP activity (ESI Fig. S8B†), suggesting that **QA** can be used for the removal of Cu even when ATRP is performed with highly active catalysts.
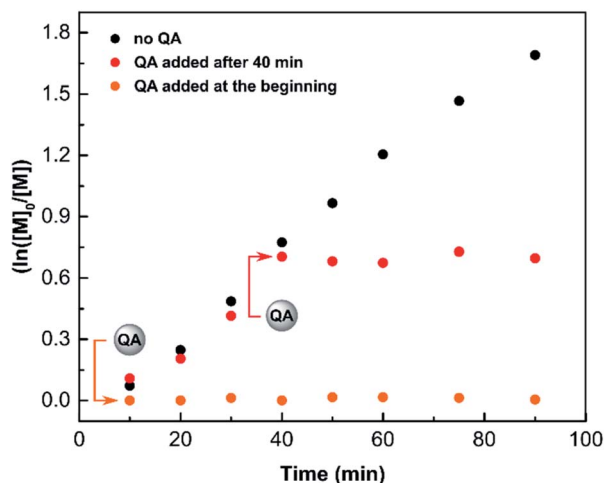

Fig. 7 Quenching of SARA ATRP by **QA**, reaction conditions: [MA]/[MBP]/[Cu^{II}Br$_2$]/[TPMA]/[QA] = 200/1/0.02/0.12/0.08, Cu^0 wire ($l = 4$ cm, $S = 1.27$ cm^2); in DMSO ([MA] = 7.4 M) at 22 °C, under anaerobic conditions.

Quenching of ATRP by QA

On a lab scale, typical ATRP quenching involves opening the post-reaction mixture to air, which provides oxidative conditions to form the deactivator Cu^{II} species. However, the amount of oxygen needed depends on the reaction volume, and thus, it cannot be scaled to industrial settings. Moreover, exposing a reaction mixture containing catalyst residues to oxidative conditions may cause undesired side products to form.[82,83] Therefore, anaerobic methods of ATRP quenching are strongly desirable.

The performance of **QA** as a quenching agent was evaluated in SARA ATRP. Methyl 2-bromopropionate (**MBP**) was used as an initiator with CuBr$_2$/TPMA/Cu(0) as the catalytic system. The reaction was carried out in DMSO with [MA]/[MBP]/[Cu^{II}Br$_2$]/[TPMA]/[QA] molar ratios of 200/1/0.02/0.12/0.08 in the presence of copper wire, under anaerobic conditions (Fig. 7). After 90 min at room temperature, the conversion of methyl acrylate (**MA**) measured by ^{1}H NMR was 0%, while in the corresponding
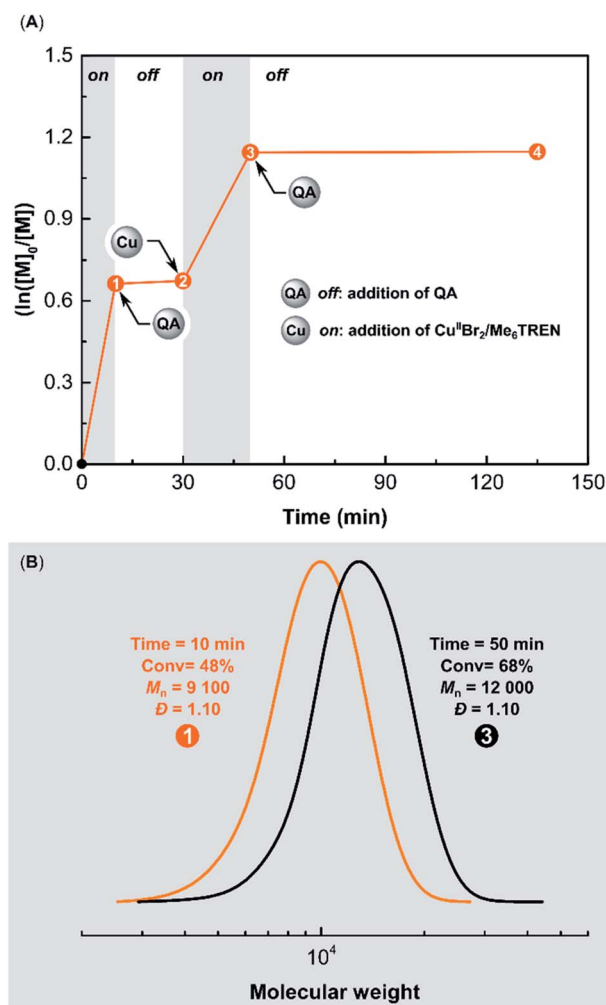

Fig. 8 (A) Kinetics of temporal control in ARGET ATRP using **QA**, reaction conditions: [MA]/[EBiB]/[Cu^{II}Br$_2$]/[Me$_6$TREN]/[AA] = 200/1/0.05/0.15/0.25 in DMSO ([MA] = 7.4 M) at 22 °C, in the presence of limited amounts of air (without degassing of DMSO and **MA**). (B) SEC traces after addition of **QA** (2 equiv. with respect to Cu^{II}Br$_2$) and [Cu^{II}Br$_2$]/[Me$_6$TREN] (with a molar ratio of 0.05/0.05 respect to EBiB).

polymerization without the addition of **QA** it was 81% (Fig. 7). Furthermore, the addition of **QA** to the reaction mixture after 40 min of polymerization resulted in an immediate quenching of ATRP (Fig. 7).

Temporal control was successfully demonstrated in ARGET ATRP of **MA** using **QA**. Ethyl α-bromoisobutyrate (**EBiB**) was used as an initiator with CuBr$_2$/Me$_6$TREN/AA as the catalytic system. The polymerization was performed in DMSO at 22 °C with [MA]/[EBiB]/[Cu^{II}Br$_2$]/[Me$_6$TREN]/[AA] molar ratios of 200/1/0.05/0.15/0.25 (Fig. 8A). After 10 min, the conversion of **MA** was 48%. Size exclusion chromatography (SEC) analysis showed that the polymer had a low dispersity ($Đ = 1.10$), and a molecular weight (MW) matching theoretical value ($M_{n,th} = 8300$, $M_n = 9100$) (Fig. 8B). The addition of **QA** (2 equiv. with respect to Cu^{II}Br$_2$) immediately stopped the ATRP. No increase in monomer conversion was observed during the 20 min period after adding **QA**. Then the polymerization was switched on by adding a second batch of [Cu^{II}Br$_2$]/[Me$_6$TREN] (with a molar ratio of 0.05/0.05 respect to [EBiB]). After a 20 min period, the monomer conversion reached 68%, confirming the retention of chain-end functionality in the presence of **QA**. SEC traces showed a clear shift toward higher MWs ($M_n = 12\,000$, $Đ = 1.10$) after restarting the ATRP, verifying a well-controlled polymerization (Fig. 8B).

Removal of copper residues after ATRP

The purification of the polymers consisted of the addition of a solution of **QA** (4 equiv.) in THF once the reaction was complete, followed by filtration using a syringe filter (0.2 μm). **QA** proved to be highly effective at removing metal residues after ATRP, usually reducing the copper content to a level below 2 ppm (Table 2). In control experiments without **QA**, metal contamination remained above 10 ppm. In extreme cases, it was over 50 times higher, up to 525 ppm (Table 2, entry 3). Additionally, the new purification protocol proved to be compatible with various monomers and ATRP techniques, including ARGET, SARA, and pATRP. The use of **QA** did not affect the molecular weight or dispersity of the purified polymers.

Preventing post-ATRP glaser coupling using QA

Azide–alkyne Huisgen cycloaddition (CuAAC) in combination with ATRP allows the synthesis of strictly defined, tailored polymers with various architectures,[84–88] especially macrocyclic

Table 2 Removal of Cu residues after ATRP[a]
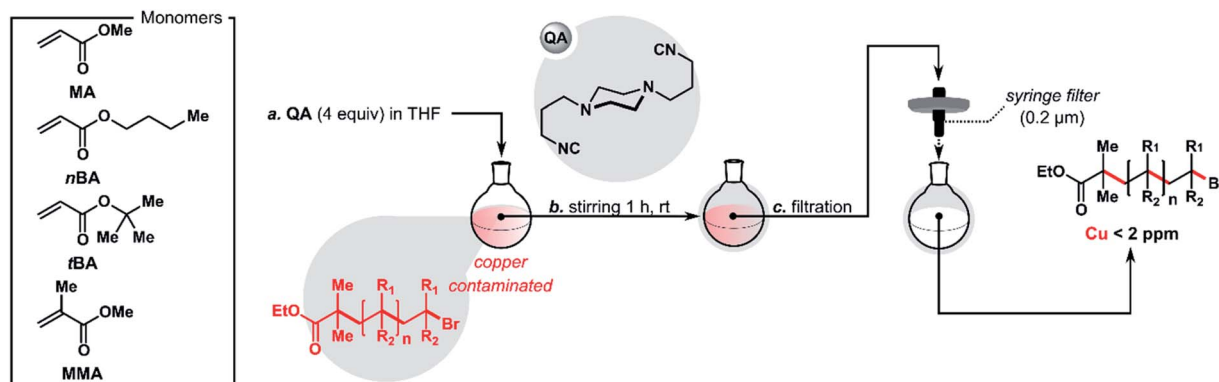
No.	Monomer	ATRP[a]	Time (h)	α[b] (%)	$M_{n,th}$[c]	$M_{n,GPC}$[d]	$Đ$[d]	QA[e] (equiv.)	Cu[f] (ppm)
1[g]	MA	ARGET	3	68	11 900	12 400	1.05	—	26.7
2[g]	MA	ARGET	3	68	11 900	13 800	1.03	4	1.38
3[h]	MA	SARA	3	90	15 700	15 400	1.05	—	525
4[h]	MA	SARA	3	85	14 800	14 400	1.07	4	0.97
5[i]	MA	pATRP	3	80	14 000	13 100	1.05	—	51.6
6[i]	MA	pATRP	3	79	13 800	13 600	1.04	4	0.91
7[j]	MA	pATRP	5	77	13 500	15 400	1.08	4	0.80
8[g]	nBA	ARGET	24	86	22 200	21 600	1.05	4	2.20
9[j]	nBA	pATRP	5	65	16 900	14 200	1.04	4	1.41
10[j]	tBA	pATRP	5	81	21 000	18 500	1.18	4	0.71
11[g]	MMA	ARGET	10	90	18 100	17 100	1.24	4	1.07

[a] Reaction conditions: [monomer]/[EBiB]/[Cu^{II}Br$_2$]/[Me$_6$TREN] = 200/1/0.05/0.25 in MeCN, ([MA] = 7.4 M, [nBA] = 4.7 M, [tBA] = 4.6 M, [MMA] = 6.2 M) at 22 °C. [b] Monomer conversion was determined by using ^{1}H NMR spectroscopy. [c] Theoretical molecular weight was calculated using the equation $M_{n,th} = [M] \times MW_M \times \alpha + MW_{EBiB}$, where [M], MW_M, α, and MW_{EBiB} correspond to initial monomer concentration, molar mass of monomer, conversion, and molar mass of EBiB initiator, respectively. [d] Molecular weight and dispersity ($Đ$) were determined by GPC analysis (THF as eluent) calibrated to poly(methyl methacrylate) standards. [e] Equivalents of QA with respect to Cu^{II}Br$_2$. [f] Copper content was determined by ICP-MS. [g] ARGET ATRP: ascorbic acid (5 equiv. with respect to Cu^{II}Br$_2$), under anaerobic conditions. [h] SARA ATRP: 4 cm Cu(0) wire ($d = 1$ mm, $S = 1.27$ cm^2), under anaerobic conditions. [i] pATRP: UV irradiation ($\lambda = 365$ nm), under anaerobic conditions. [j] pATRP: UV irradiation ($\lambda = 365$ nm), in the presence of limited amounts of air (without degassing of MeCN and monomer).

polymers that are difficult to prepare by other methods.[89] This synthetic route involves the preparation of a linear precursor with a terminal alkyne group by ATRP, followed by the nucleophilic displacement of the bromide chain end with azide and finally CuAAC-mediated macrocyclization reaction at high dilution. However, during these transformations, side reactions can occur that compromise the fidelity of the chain end, such as (i) radical termination at high monomer conversions and (ii) Glaser coupling of the alkyne moiety under oxidative conditions.[90] Both side reactions jeopardize the subsequent CuAAC-mediated macrocyclization.

While the conventional radical termination can be minimized by decreasing the rate of polymerization and by terminating the reaction at lower monomer conversion, suppression of the Glaser coupling remains a challenge.[82,91,92] One of the methods of preventing the Glaser coupling is the protection of the alkyne group with a trimethylsilyl or triisopropylsilyl group.[93] However, this approach requires an additional protection/deprotection sequence, which has a low atom and time economy. In addition, the deprotection step requires the use of reagents that can cause the degradation of the synthesized polymer.

Recently, in an inspiring work, Koberstein and co-workers showed two methods for preventing post-ATRP alkyne–alkyne coupling.[82] First, Glaser coupling can be completely prevented by cooling the post-reaction mixture below −28 °C before exposing it to air and then maintaining a low temperature during the polymer workup. Second, the coupling is suppressed by the use of an excess of reducing agents, such as tin(ɪɪ) 2-ethylhexanoate or (+)-sodium ʟ-ascorbate. Moreover, it was found that high-denticity ligands can reduce Glaser coupling rates. However, the proposed approaches are difficult to scale up because of the necessity of using aluminum oxide during the purification process. For this reason, the development of economical and simple methods of preventing oxidative alkyne–alkyne coupling is desirable.
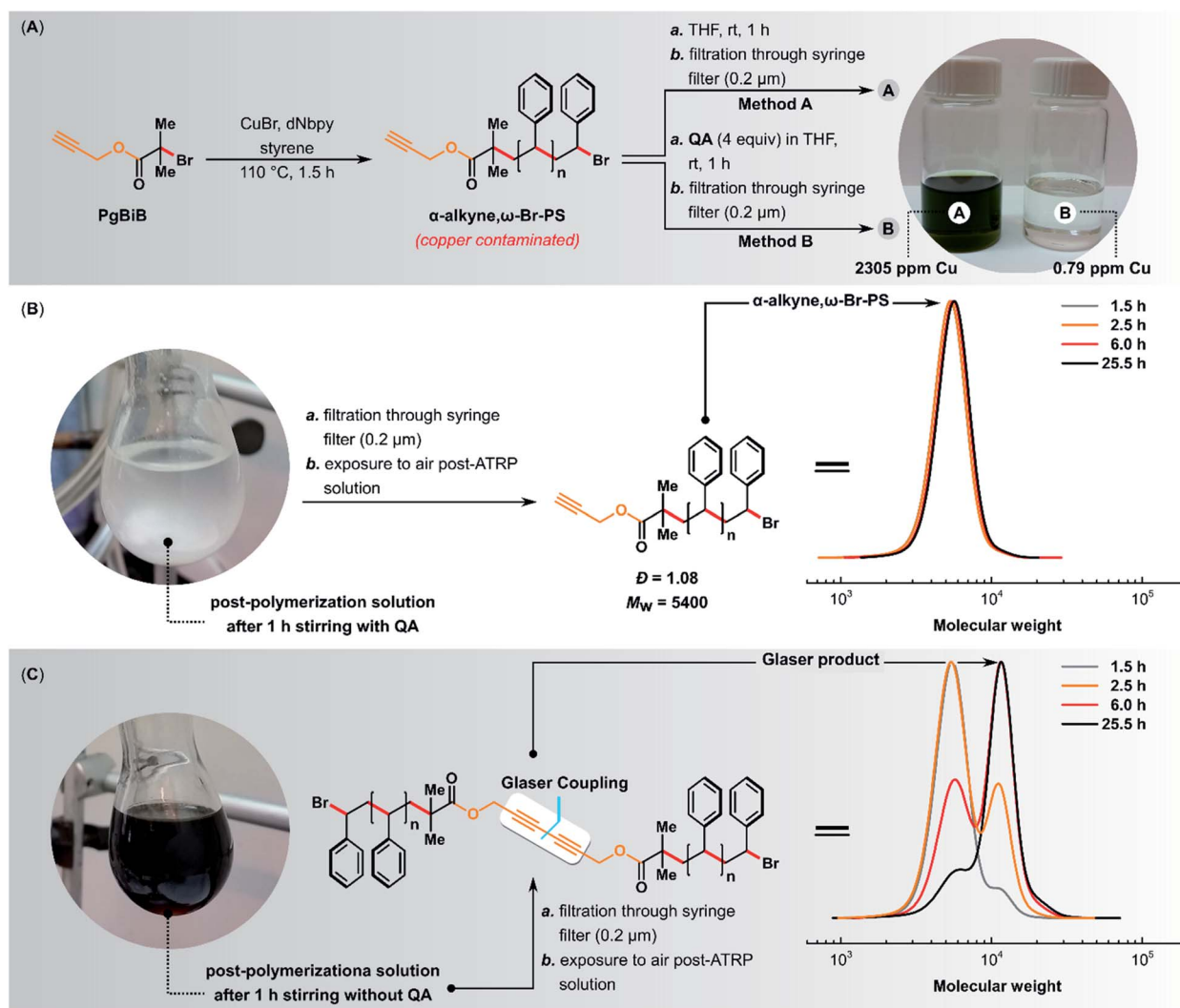

Fig. 9 (A) Preventing post-ATRP Glaser coupling using **QA**. Normal ATRP of styrene, reaction conditions: [styrene]/[PgBiB]/[Cu^{I}Br]/[dNbpy] = 1/1/2/230 in bulk at 110 °C. (B) Exposure to air post-ATRP mixture after the addition of **QA** (4 equiv. with respect to Cu^{I}Br). (C) Exposure to air post-ATRP mixture without the addition of **QA**.

The linear polystyrene (α-alkyne,ω-Br-PS) was prepared using standard ATRP. 3-Butynyl 2-bromoisobutyrate (**PgBiB**) was used as initiator with CuBr/dNbpy (dNbpy = 4,4′-dinonyl-2,2′-bipyridine) as the catalyst system. The reaction was carried out in bulk at 110 °C with [styrene]/[PgBiB]/[Cu^{I}Br]/[dNbpy] molar ratios of 230/1/1/2. After 1.5 h, two samples of 4.5 mL each were taken from the reaction mixture and purified using method A or B (Fig. 9A).

The addition of **QA** (4 equiv. with respect to Cu^{I}Br) to the post-ATRP reaction mixture not only completely prevented the Glaser coupling (*i.e.*, the average molecular weight of the polymer did not change over time when the mixture was exposed to air) but also caused the quantitative precipitation of the copper(I) complex with the **QA** ligand (Fig. 9B). The complex was easily removed by simple filtration, giving a colorless polymer with copper content below 1 ppm and low Đ (1.08). In the control experiment in which **QA** was not added, the average molecular weight and Đ of the resulting polymer increased over time (Fig. 9C), and the obtained polymer had an intense color and a very high copper content of 2305 ppm.

Fig. 10 The cytotoxicity assay performed using HEK293 (black) and NIH3T3 cells (orange). Cells were treated with five concentrations of **QA** or **HQA** for 72 hours and compared to control group (no treatment). Bars indicate the mean percent viability ± SEM ($n = 3$), ns: no significant difference, *$p < 0.5$, **$p < 0.01$, ***$p < 0.001$ (*vs.* control group).

Cytotoxicity study of QA

Finally, we investigated the cytotoxicity of **QA** and its acidic hydrolysis product **HQA** (*N,N′*-(piperazine-1,4-diylbis(propane-3,1-diyl))diformamide). **HQA** was obtained by adding 4 equiv. of HCl to **QA** dissolved in water and stirring for 2 hours. The resulting solution was diluted in buffer to the desired concentration without isolating **HQA** (Fig. 10). To ensure that hydrolysis was quantitative, the same procedure was performed in D$_2$O and monitored by ^{1}H NMR spectroscopy. After 2 hours, no peaks from **QA** were visible in the spectrum.

The toxicity study was performed using two different cell lines: HEK293 (human embryonic kidney cells) and NIH3T3 (mouse fibroblast cells). **QA** and **HQA** were tested at five different concentrations (Fig. 10). The cells were tolerant to 0.01 μM of either of the compounds up to 72 hours. However, at concentrations above 0.01 μM, **QA** started exhibiting cytotoxicity in a time-dependent manner (ESI Fig. S9†) in both cell lines. The highest level of cytotoxicity of **QA** was observed at 72 hours, with approximately 50% of cells remaining viable after treatment with 10 μM **QA** compared to the control (no treatment) group. On the other hand, **HQA** was not cytotoxic even at 10 μM, suggesting that acidic hydrolysis of **QA** is an effective way to neutralize its toxicity.

Conclusions

In this study, we have shown that **QA** is a rapid quenching agent for Stahl oxidation and ATRP, as well as a highly efficient Cu scavenger. The use of a small amount of silica gel in combination with a small excess of **QA** reduced the Cu content in aldehydes below 5 ppm. This purification protocol was effective on a gram scale in the synthesis of the cardiovascular disease drug precursor (rosuvastatin), leading to a product containing only 3.6 ppm Cu.

Spectroscopic and electrochemical studies provided insights into the reactivity of **QA** toward Cu complexes used as ATRP catalysts and showed that **QA** is highly reactive against Cu^I/L, even for ligands with very high copper binding constants (10^{13} M^{-1}). At the same time, **QA** proved to be inert towards Cu^{II}/L complexes with strong σ-donor ligands. However, the use of a reducing agent allowed **QA** to bind copper quantitatively.

QA very efficiently removed Cu after ATRP without compromising the molecular weight and dispersity of the purified polymers. The addition of **QA** followed by simple filtration using a syringe filter proved to be highly effective in removing Cu contamination, affording polymers with Cu content below 2 ppm. This protocol was of great significance for normal ATRP, leading to polystyrene with less than 1 ppm Cu. Treatment with **QA** not only facilitated the removal of Cu, but also completely prevented the Glaser coupling under oxidative conditions.

Finally, we examined the cytotoxicity of **QA**. The isocyanide showed moderate cytotoxicity, with approximately 50% of cells remaining viable after 72 hours of treatment with 10 μM of the compound. However, it could be easily hydrolyzed by adding a small excess of HCl. The hydrolysis product showed no cytotoxicity even at relatively high concentrations.
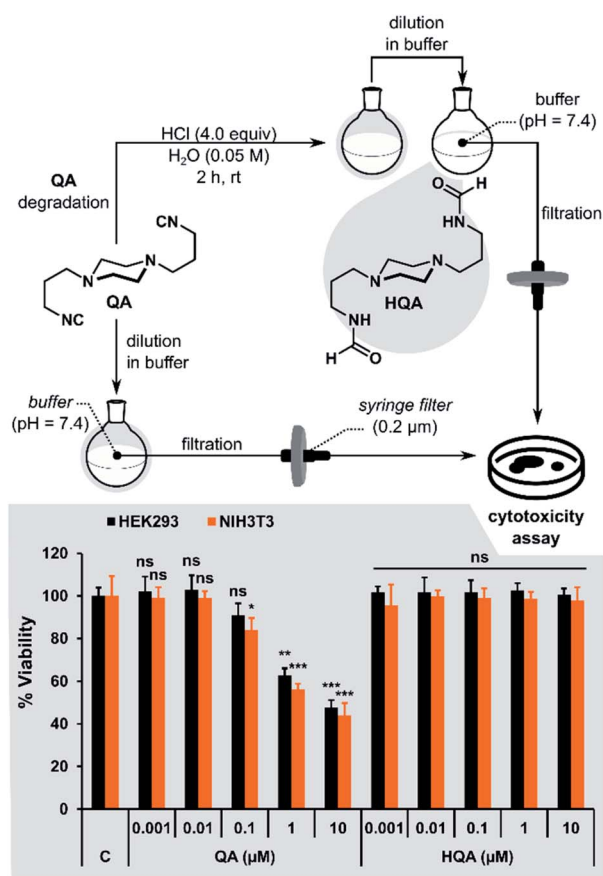
In summary, we presented the applicability of **QA** in two fundamental reactions catalyzed by copper complexes. We expect this straightforward approach to find application in other significant transformations catalyzed by transition metal complexes.

Conflicts of interest

There are no conflicts to declare.

Acknowledgements

References

1 P. Ruiz-Castillo and S. L. Buchwald, *Chem. Rev.*, 2016, **116**, 12564–12649.

2 D. Wang and D. Astruc, *Chem. Rev.*, 2015, **115**, 6621–6686.

3 C. C. C. Johansson Seechurn, M. O. Kitching, T. J. Colacot and V. Snieckus, *Angew. Chem., Int. Ed.*, 2012, **51**, 5062–5085.

4 H. Li, C. C. C. Johansson Seechurn and T. J. Colacot, *ACS Catal.*, 2012, **2**, 1147–1164.

5 R. H. Grubbs, *Angew. Chem., Int. Ed.*, 2006, **45**, 3760–3765.

6 P. O'Brien, *Angew. Chem., Int. Ed.*, 1999, **38**, 326–329.

7 S. H. Hong, D. P. Sanders, C. W. Lee and R. H. Grubbs, *J. Am. Chem. Soc.*, 2005, **127**, 17160–17161.

8 Ö. Usluer, M. Abbas, G. Wantz, L. Vignau, L. Hirsch, E. Grana, C. Brochon, E. Cloutet and G. Hadziioannou, *ACS Macro Lett.*, 2014, **3**, 1134–1138.

9 C. S. Higman, J. A. M. Lummiss and D. E. Fogg, *Angew. Chem., Int. Ed.*, 2016, **55**, 3552–3565.

10 J. Magano and J. R. Dunetz, *Chem. Rev.*, 2011, **111**, 2177–2250.

11 C. A. Busacca, D. R. Fandrick, J. J. Song and C. H. Senanayake, *Adv. Synth. Catal.*, 2011, **353**, 1825–1864.

12 E. J. Flahive, B. L. Ewanicki, N. W. Sach, S. A. O'Neill-Slawecki, N. S. Stankovic, S. Yu, S. M. Guinness and J. Dunn, *Org. Process Res. Dev.*, 2008, **12**, 637–645.

13 P. Wheeler, J. H. Phillips and R. L. Pederson, *Org. Process Res. Dev.*, 2016, **20**, 1182–1190.

14 G. Szczepaniak, K. Kosiński and K. Grela, *Green Chem.*, 2014, **16**, 4474–4492.

15 G. C. Vougioukalakis, *Chem.–Eur. J.*, 2012, **18**, 8868–8880.

16 B. R. Galan, K. P. Kalbarczyk, S. Szczepankiewicz, J. B. Keister and S. T. Diver, *Org. Lett.*, 2007, **9**, 1203–1206.

17 G. Szczepaniak, K. Urbaniak, C. Wierzbicka, K. Kosiński, K. Skowerski and K. Grela, *ChemSusChem*, 2015, **8**, 4139–4148.

18 G. Szczepaniak, A. Ruszczyńska, K. Kosiński, E. Bulska and K. Grela, *Green Chem.*, 2018, **20**, 1280–1289.

19 G. Szczepaniak, W. Nogaś, J. Piątkowski, A. Ruszczyńska, E. Bulska and K. Grela, *Org. Process Res. Dev.*, 2019, **23**, 836–844.

20 A. J. Hickman and M. S. Sanford, *Nature*, 2012, **484**, 177–185.

21 H. C. Kolb, M. G. Finn and K. B. Sharpless, *Angew. Chem., Int. Ed.*, 2001, **40**, 2004–2021.

22 K. Matyjaszewski, *Macromolecules*, 2012, **45**, 4015–4039.

23 C. Sambiagio, S. P. Marsden, A. J. Blacker and P. C. McGowan, *Chem. Soc. Rev.*, 2014, **43**, 3525–3550.

24 S. E. Allen, R. R. Walvoord, R. Padilla-Salinas and M. C. Kozlowski, *Chem. Rev.*, 2013, **113**, 6234–6458.

25 V. P. Boyarskiy, N. A. Bokach, K. V. Luzyanin and V. Y. Kukushkin, *Chem. Rev.*, 2015, **115**, 2698–2779.

26 B. L. Ryland and S. S. Stahl, *Angew. Chem., Int. Ed.*, 2014, **53**, 8824–8838.

27 C. Parmeggiani and F. Cardona, *Green Chem.*, 2012, **14**, 547.

28 A. J. Mancuso and D. Swern, *Synthesis*, 1981, **1981**, 165–185.

29 J. R. Parikh and W. v. E. Doering, *J. Am. Chem. Soc.*, 1967, **89**, 5505–5507.

30 S. Wertz and A. Studer, *Green Chem.*, 2013, **15**, 3116.

31 Q. Cao, L. M. Dornan, L. Rogan, N. L. Hughes and M. J. Muldoon, *Chem. Commun.*, 2014, **50**, 4524–4543.

32 J. M. Hoover, J. E. Steves and S. S. Stahl, *Nat. Protoc.*, 2012, **7**, 1161–1166.

33 J. M. Hoover and S. S. Stahl, *J. Am. Chem. Soc.*, 2011, **133**, 16901–16910.

34 R. C. Walroth, K. C. Miles, J. T. Lukens, S. N. MacMillan, S. S. Stahl and K. M. Lancaster, *J. Am. Chem. Soc.*, 2017, **139**, 13507–13517.

35 S. D. McCann and S. S. Stahl, *Acc. Chem. Res.*, 2015, **48**, 1756–1766.

36 J. F. Greene, J. M. Hoover, D. S. Mannel, T. W. Root and S. S. Stahl, *Org. Process Res. Dev.*, 2013, **17**, 1247–1251.

37 A. Ochen, R. Whitten, H. E. Aylott, K. Ruffell, G. D. Williams, F. Slater, A. Roberts, P. Evans, J. E. Steves and M. J. Sanganee, *Organometallics*, 2019, **38**, 176–184.

38 B. L. Ryland, S. D. McCann, T. C. Brunold and S. S. Stahl, *J. Am. Chem. Soc.*, 2014, **136**, 12166–12173.

39 K. Matyjaszewski, *Adv. Mater.*, 2018, **30**, 1706441.

40 K. Matyjaszewski and N. V. Tsarevsky, *J. Am. Chem. Soc.*, 2014, **136**, 6513–6533.

41 K. Matyjaszewski and N. V. Tsarevsky, *Nat. Chem.*, 2009, **1**, 276–288.

42 F. di Lena and K. Matyjaszewski, *Prog. Polym. Sci.*, 2010, **35**, 959–1021.
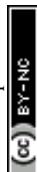
43 T. E. Patten, J. Xia, T. Abernathy and K. Matyjaszewski, *Science*, 1996, **272**, 866–868.

44 J.-S. Wang and K. Matyjaszewski, *J. Am. Chem. Soc.*, 1995, **117**, 5614–5615.

45 W. Jakubowski, K. Min and K. Matyjaszewski, *Macromolecules*, 2006, **39**, 39–45.

46 W. Jakubowski and K. Matyjaszewski, *Angew. Chem., Int. Ed.*, 2006, **45**, 4482–4486.

47 K. Matyjaszewski, W. Jakubowski, K. Min, W. Tang, J. Huang, W. A. Braunecker and N. V. Tsarevsky, *Proc. Natl. Acad. Sci. U. S. A.*, 2006, **103**, 15309–15314.

48 D. Konkolewicz, Y. Wang, M. Zhong, P. Krys, A. A. Isse, A. Gennaro and K. Matyjaszewski, *Macromolecules*, 2013, **46**, 8749–8772.

49 A. J. D. Magenau, N. C. Strandwitz, A. Gennaro and K. Matyjaszewski, *Science*, 2011, **332**, 81–84.

50 D. Konkolewicz, K. Schröder, J. Buback, S. Bernhard and K. Matyjaszewski, *ACS Macro Lett.*, 2012, **1**, 1219–1223.

51 H. Mohapatra, M. Kleiman and A. P. Esser-Kahn, *Nat. Chem.*, 2017, **9**, 135–139.

52 Z. Wang, Z. Wang, X. Pan, L. Fu, S. Lathwal, M. Olszewski, J. Yan, A. E. Enciso, Z. Wang, H. Xia and K. Matyjaszewski, *ACS Macro Lett.*, 2018, **7**, 275–280.

53 E. H. Discekici, A. Anastasaki, J. Read de Alaniz and C. J. Hawker, *Macromolecules*, 2018, **51**, 7421–7434.

54 N. J. Treat, H. Sprafke, J. W. Kramer, P. G. Clark, B. E. Barton, J. Read de Alaniz, B. P. Fors and C. J. Hawker, *J. Am. Chem. Soc.*, 2014, **136**, 16096–16101.

55 X. Pan, C. Fang, M. Fantin, N. Malhotra, W. Y. So, L. A. Peteanu, A. A. Isse, A. Gennaro, P. Liu and K. Matyjaszewski, *J. Am. Chem. Soc.*, 2016, **138**, 2411–2425.

56 J. C. Theriot, C.-H. Lim, H. Yang, M. D. Ryan, C. B. Musgrave and G. M. Miyake, *Science*, 2016, **352**, 1082–1086.

57 G. Xie, M. R. Martinez, M. Olszewski, S. S. Sheiko and K. Matyjaszewski, *Biomacromolecules*, 2019, **20**, 27–54.

58 D. C. Kennedy, C. S. McKay, M. C. B. Legault, D. C. Danielson, J. A. Blake, A. F. Pegoraro, A. Stolow, Z. Mester and J. P. Pezacki, *J. Am. Chem. Soc.*, 2011, **133**, 17993–18001.

59 N. Jasinski, A. Lauer, P. J. M. Stals, S. Behrens, S. Essig, A. Walther, A. S. Goldmann and C. Barner-Kowollik, *ACS Macro Lett.*, 2015, **4**, 298–301.

60 M. Ding, X. Jiang, L. Zhang, Z. Cheng and X. Zhu, *Macromol. Rapid Commun.*, 2015, **36**, 1702–1721.

61 Y. Shen, H. Tang and S. Ding, *Prog. Polym. Sci.*, 2004, **29**, 1053–1078.

62 H.-C. Lee, M. Fantin, M. Antonietti, K. Matyjaszewski and B. V. K. J. Schmidt, *Chem. Mater.*, 2017, **29**, 9445–9455.

63 H.-C. Lee, M. Antonietti and B. V. K. J. Schmidt, *Polym. Chem.*, 2016, **7**, 7199–7203.

64 G. Kickelbick, H. Paik and K. Matyjaszewski, *Macromolecules*, 1999, **32**, 2941–2947.

65 Y. Wang, F. Lorandi, M. Fantin, P. Chmielarz, A. A. Isse, A. Gennaro and K. Matyjaszewski, *Macromolecules*, 2017, **50**, 8417–8425.

66 B. Zhang, L. Yao, X. Liu, L. Zhang, Z. Cheng and X. Zhu, *ACS Sustainable Chem. Eng.*, 2016, **4**, 7066–7073.

67 M. E. Honigfort, W. J. Brittain, T. Bosanac and C. S. Wilcox, *Macromolecules*, 2002, **35**, 4849–4851.

68 M. F. Ebbesen, D. Itskalov, M. Baier and L. Hartmann, *ACS Macro Lett.*, 2017, **6**, 399–403.

69 X. Su, P. G. Jessop and M. F. Cunningham, *Macromolecules*, 2018, **51**, 8156–8164.

70 K. Matyjaszewski, T. Pintauer and S. Gaynor, *Macromolecules*, 2000, **33**, 1476–1478.

71 A. J. D. Magenau, N. Bortolamei, E. Frick, S. Park, A. Gennaro and K. Matyjaszewski, *Macromolecules*, 2013, **46**, 4346–4353.

72 F. Canturk, B. Karagoz and N. Bicak, *J. Polym. Sci., Part A: Polym. Chem.*, 2011, **49**, 3536–3542.

73 J. M. Blacquiere, T. Jurca, J. Weiss and D. E. Fogg, *Adv. Synth. Catal.*, 2008, **350**, 2849–2855.

74 J. E. Steves and S. S. Stahl, *J. Org. Chem.*, 2015, **80**, 11184–11188.

75 J. E. Steves and S. S. Stahl, *J. Am. Chem. Soc.*, 2013, **135**, 15742–15745.

76 J. E. Steves, Y. Preger, J. R. Martinelli, C. J. Welch, T. W. Root, J. M. Hawkins and S. S. Stahl, *Org. Process Res. Dev.*, 2015, **19**, 1548–1553.

77 T. G. Ribelli, F. Lorandi, M. Fantin and K. Matyjaszewski, *Macromol. Rapid Commun.*, 2019, **40**, 1800616.

78 N. Bortolamei, A. A. Isse, V. B. Di Marco, A. Gennaro and K. Matyjaszewski, *Macromolecules*, 2010, **43**, 9257–9267.

79 A. A. Isse, F. Lorandi and A. Gennaro, *Curr. Opin. Electrochem.*, 2019, **15**, 50–57.

80 C. P. Andrieux, C. Blocman, J. M. Dumas-Bouchiat, F. M'Halla and J. M. Savéant, *J. Electroanal. Chem. Interfacial Electrochem.*, 1980, **113**, 19–40.

81 K. Schröder, R. T. Mathers, J. Buback, D. Konkolewicz, A. J. D. Magenau and K. Matyjaszewski, *ACS Macro Lett.*, 2012, **1**, 1037–1040.

82 P. Leophairatana, S. Samanta, C. C. De Silva and J. T. Koberstein, *J. Am. Chem. Soc.*, 2017, **139**, 3756–3766.

83 W. P. Gallagher and A. Vo, *Org. Process Res. Dev.*, 2015, **19**, 1369–1373.

84 S. Zhang, T. Vi, K. Luo and J. T. Koberstein, *Macromolecules*, 2016, **49**, 5461–5474.

85 H. Gao and K. Matyjaszewski, *J. Am. Chem. Soc.*, 2007, **129**, 6633–6639.

86 J. A. Johnson, D. R. Lewis, D. D. Díaz, M. G. Finn, J. T. Koberstein and N. J. Turro, *J. Am. Chem. Soc.*, 2006, **128**, 6564–6565.

87 M. A. White, J. A. Johnson, J. T. Koberstein and N. J. Turro, *J. Am. Chem. Soc.*, 2006, **128**, 11356–11357.

88 N. V. Tsarevsky, B. S. Sumerlin and K. Matyjaszewski, *Macromolecules*, 2005, **38**, 3558–3561.

89 B. A. Laurent and S. M. Grayson, *J. Am. Chem. Soc.*, 2006, **128**, 4238–4239.

90 P. Siemsen, R. C. Livingston and F. Diederich, *Angew. Chem., Int. Ed.*, 2000, **39**, 2632–2657.

91 P. Leophairatana, C. C. De Silva and J. T. Koberstein, *J. Polym. Sci., Part A: Polym. Chem.*, 2018, **56**, 75–84.

92 C. J. Duxbury, D. Cummins and A. Heise, *J. Polym. Sci., Part A: Polym. Chem.*, 2009, **47**, 3795–3802.

93 W. K. Storms-Miller and C. Pugh, *Macromolecules*, 2015, **48**, 3803–3810.